Rev. Roum. Sci. Techn.– Électrotechn. et Énerg.
Vol. **65**, *3–4*, pp. 191–198, Bucarest, 2020

LIGHTNING PERFORMANCE OF HIGH VOLTAGE OVERHEAD LINES ASSESSED USING THE CRITICAL CURRENTS CURVES

ILEANA BARAN[1], COSTEA MARIAN[1], TUDOR LEONIDA[1], CRISTINA MIRELA MICU[2]

Keywords: Lightning protection, Insulation flashover, Critical current, Total flashover rate, Line surge arrester.

The paper introduces the concept of critical currents curve and uses it to assess the lightning performance of high voltage overhead lines. The line total flashover rate (N_D) was selected to qualify the lightning performance of the line. The method developed to evaluate the line total flashover rate is a combination between numerical simulation in ATP-EMTP (which compute the voltage applied to the insulator strings during a lightning strike), and dedicated statistical techniques conceived to evaluate the occurrence probabilities for flashover or back flashover events. The method can be applied to establish an order of merit among different solutions intended to improve the lightning protection of the line, including line surge arresters (LSA).

1. INTRODUCTION

For most overhead power transmission lines (OHL), lightning is the primary cause of unscheduled interruptions. Several methods for estimating OHL flashover rate due to lightning events have been developed in the past, and many publications have been written on how to design transmission lines that experience a minimum number of interruptions [1–3]. More recently, international pre-normative institutions, such as IEEE and CIGRE, have paid great interest to the subject, and extensive overview work was developed by several working groups [4, 5]. This work led to guidelines for estimating the lightning performance of transmission lines which are internationally accepted [6, 7]. The methods mentioned above have been developed for OHL protected against lightning with grounding wires and for that reason, they generally cannot be used to assess the effectiveness of modern lightning protection solutions which use line surge arresters (LSA), especially in areas with high values of earth electrical resistivity such as mountainous regions, [9,10].

The paper proposes a novel estimation method of the OHL total flashover rate (N_D), applicable for any actual state of the OHL fitting. The method combines (i) a deterministic part consisting in the computation of the fast front overvoltages which stress the line's insulation in different scenarios of striking using ATP-EMTP, and (ii) a stochastic part based on statistical distribution laws of lightning current parameters, aimed to evaluate the intrinsic probability of having a disruptive discharge as the response of the line's insulation to an overvoltage generated by a lightning current with known crest value and shape.

2. PRELIMINARY STAGES IN THE ASSESSMENT OF THE TOTAL FLASHOVER RATE

The evaluation of the total flashover rate (N_D) requires the completion of several preliminary steps, outlined below.

a) – Technical data regarding the line and its supportive structures. The lightning performance of an overhead line (OHL) depends on several structural characteristics such as towers geometry, phase equipping, insulation level provide by insulator strings, tower grounding (artificial or natural), the average value of the tower footing resistance. All these different categories of information should be addressed and made available for the analysis purposes.

b) – Regional value of the ground flash density, GFD in flashes/km^2/year is defined as the number of cloud-to-ground flashes occurring during a year over an area equal to 1 km^2. GFD is considered as the primary descriptor of lightning activity, at least in lightning protection studies. Local values of GFD can be estimated using lightning location systems data, where available. If the region of interest is not covered by a network able to detect and locate cloud-to-ground flashes, an estimate of the GFD can be obtained using actual values of the annual number of thunderstorm days *TD*, known also as keraunic level. For now, the most reliable correlation between *TD* and GFD is the one proposed by Anderson in [11]:

$$\mathrm{GFD} = 0.04 \cdot TD^{1.25}. \tag{1}$$

It should be noticed that, as all lightning activity indicators, *GFD* values are of statistical nature and can vary significantly from year to year.

c) - Flashes collection rate, N_S in flashes/100km/year is defined as the annual number of lightning flashes which terminate on one of the constitutive parts of an OHL within 100 km of line. The "attractiveness" of the line can be evaluated through various models based on electro-geometrical concepts, or it can be roughly estimated using the relationship proposed in [12] and adopted by many researchers when trying to obtain an average value for N_S:

$$N_S = 0.1 GFD\left(28h^{0.6} + b\right) \tag{2}$$

where h is the tower height and b the grounding wires separation distance both in meters (h = 27.5m, b = 13.0 m).

3. CONSEQUENCES OF DIRECT STRIKES TO THE LINE'S CONSTITUTIVE PARTS

Each flash collected by the OHL will terminate, with a given probability, on one of the line's main constitutive parts, *i.e.* towers, grounding wire(s) or phase conductors, and the lightning current will begin to circulate on different paths determined by the point-of-strike location. One of the consequences of such an event is the apparition of overvoltages, designed as fast front or lightning overvoltages, which represent severe electric stress for the line's insulation, *i.e.* insulator strings and air intervals. The crest value and the shape parameters of lightning overvoltages depend upon the shape and crest value of the

[1] University Politehnica of Bucharest, ileana.baran@upb.ro, marian_costea2003@yahoo.com, tudor_l@yahoo.com
[2] Subwatt Energy Consulting SRL, micumirelacristina@gmail.com

lightning current and the location of the point-of-strike. The resulting stress may exceed the insulation level provided by insulator strings or may cause flashover between conductors and the tower structure. It should be noted that while the overvoltages are strongly correlated to the lightning current features, the insulation level is based on the rated voltage of the OHL.

a) Possible scenarios in the case of a lightning strike. A direct strike to a shielded line may terminate to a phase conductor (*shielding failure*) or to grounded parts of the line such as the top of the tower or the grounding wire(s). The overvoltage that occurs during a shielding failure will stress the phase to ground insulation in a normal way, *i.e.* the high voltage terminal being the phase conductor, and may produce a *flashover* (FO). If the strike is to a grounded part, the overvoltage occurring in any of the two possible scenarios (top of the tower or grounding wire) may cause the so-called *backflashover* (BFO), because in this case, the voltage at the insulation terminals is applied in a reverse way to the one corresponding to stress in normal duty mode: the grounded part becomes the high voltage terminal while the phase conductor becomes a lower voltage terminal. A flowchart of the models developed to evaluate the number of strikes which terminate on each part of the line is presented in Fig.1. The models have been established for a single circuit OHL with the phases arranged in a triangle, in two alternatives, with or without grounding wires. In the case of a line without grounding wires, the strikes will be distributed between the top of the tower and one of the phase conductors at midspan.

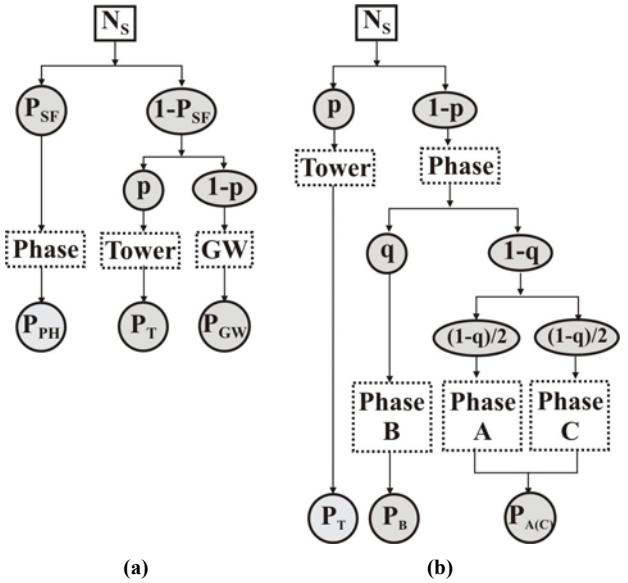

Fig.1 – Distribution of lightning strikes between different parts of a single circuit line, the flowchart showing the main stages to follow. *PH*-phase, *T*-tower, *GW*-grounding wire
(a)-OHL with grounding wire(s); (b)-OHL without grounding wire(s).

The significance of the quantities in Fig.1 is as follows: P_{SF}–the probability of shielding failure, p–the probability of having a point-of-strike to the top of a tower, (1–p)-the probability of having a point-of-strike to the grounding wire(s) at midspan, q–the probability of having a point-of-strike at midspan on the central phase (B), (1–q)-the probability of having a point-of-strike at midspan on one of the lateral phases A(C). All the quantities listed above can be evaluated using available electrogeometric models or empirical relationships.

Not every strike terminated on a line part will result in a disruptive discharge (FO or BFO event). Therefore, the flowchart in Fig.1 contains a set of quantities intended to express the probability of having a FO or a BFO in each of the resulting scenarios, namely: P_{PH} – the probability of FO in case of shielding failure, P_T–the probability of BFO for a point-of-strike to the top of a tower, P_{GW}-the probability of BFO for a point-of-strike at midspan on a grounding wire(s), P_B or $P_{A(C)}$–the probability of FO for a point-of-strike at midspan on the central or lateral phases respectively. All these probabilities are decided by the response of the phase-to-ground insulation to the crest value and the shape of the overvoltages generated during the strike event.

b) Insulation response to lightning overvoltages. As previously pointed out, the waveform of the voltage at insulation terminals during a return stroke event, depends largely on the waveform of the lightning current. But, the procedures applied to achieve insulation coordination stipulate the standard lightning impulse voltage (LI) 1.2/50 μs as the representative waveform for the short-front (lightning) overvoltages. The response of the OHL insulation to this type of stress can be specified using two characteristics: (i) the discharge probability function $P_d\,(U_{crest})$, which gives the correlation between the discharge probability P_d and the crest value of the applied voltage U_{crest}, and (ii) the volt-time characteristic $U_d\,(T_d)$, which connects the disruptive voltage at the insulation terminals U_d to the time to flashover T_d . A fictitious voltage-time characteristic is represented in Fig.2 to illustrate the use of specific terms. The discharge probability function for LI is described by the equation of the normal cumulative distribution function which in turn is completely specified by two parameters: ($U50$ or CFO) the lightning critical flashover voltage defined as the crest value of a standard lightning impulse for which the insulation exhibits 50 % withstand probability, and Z the standard deviation of $P_d\,(U_{crest})$.

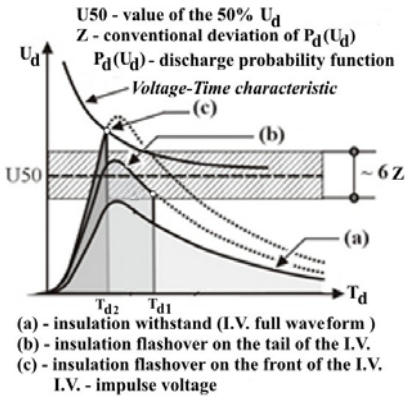

Fig. 2 – Voltage – time-to-flashover characteristic ($U_d\,(T_d)$), a qualitative description.

In insulation coordination practice, parameters $U50$ and Z are sufficient to assess the required insulation performance to short-front impulses. But, when dealing with OHL lightning protection, we are interested to establish the minimal critical conditions leading to a flashover for voltage impulses with rising speeds much higher than that corresponding to LI. Therefore, the volt-time characteristic is a tool frequently used in procedures meant to evaluate the flashover rate. It should be noted that experimentally obtaining such a feature is not easy, which is why available information is scarce.

Nevertheless, a version of U_d (T_d) obtained as an average of results accessible at different laboratories is given in [18]:

$$U_d = \left(400 + 710/T_d^{0.75}\right) \cdot L_{string} \qquad U_d\,[\text{kV}],\ T_d\,[\mu\text{s}],\ L_{string}\,[\text{m}] \tag{3}$$

where L_{string} is the length of the insulator string. The volt-time curve in (3) tends to flatten out at about 16 μs, the asymptotic value being equal to the CFO. The critical current was defined and evaluated in the following using this volt-time curve. It must be noticed that the volt-time curve in (3) is currently used for both polarities, thus neglecting the effect of polarity on the disruptive voltage.

4. LIGHTNING PARAMETERS FOR FLASHOVER

A summary of lightning parameters that make their mark on the features of the overvoltages associated with a strike will be presented in this section; for other references see [13, 14].

a) Flash development and polarity. The lightning flashes can be classified using two criteria: the polarity of the electric charge transferred to ground (positive or negative), and the direction of propagation from the initiation to the strike point (downward and upward). *Downward flashes* are initiated inside the cloud by a precursor leader which propagates downward from cloud to ground, while *upward flashes* are initiated by an upward leader from a grounded structure which propagates towards the cloud. Downward flashes usually occur in the flat territory and to lower grounded structures, while upward flashes become dominant as the effective height of the structures increases. In practice, the majority of OHL does not involve structures of sufficient height to initiate upward flashes. From the observed polarity of the charge transferred to the ground, about 90 % of the downward flashes are negative. Accordingly, the analysis that follows will be restrained to negative downward flashes.

b) Number of strokes per flash. Negative downward flashes can include multiple strokes: the first stroke followed by one or several subsequent strokes. The proportion of single stroke negative downward flashes reported by different authors have been summarized in [15], and varies between 13 % and 76 %, with an overall combined results value equal to 45 %. The mean number of strokes per flash varies between 1.9 and 4.2 with an overall combined results value equal to 3.1 strokes in a flash. The considerable dispersion of the observed values arises out mainly due to the variety of measuring methods adopted.

c) Return stroke current's waveform. Each stroke in a lightning flash consists of a sequence of leader/return stroke stages. During each of the *return stroke* stages of a lightning flash (first or subsequent), the discharge channel and the grounded parts connected to it through the point-of-strike become the path for current circulation. Lightning stroke currents differ in shape and amplitude due to the stochastic character of the lightning events.

A current's waveform typical for the first stroke of a negative downward flash is represented in Fig. 3. The figure contains also the main parameters describing the front of the waveform with their commonly used names and definitions; the figure has been adapted from [15]. In brief, for the first and subsequent strokes, the waveform parameters of the current are:

- two parameters describing the front duration: $T_{10/90}$ expressed as the interval between 10 and 90 % amplitude intercepts on the front and $T_{30/90}$ expressed as the interval between 30 and 90 % intercepts;
- the average current steepness between 10 and 90 % amplitude intercepts defined as $S_{10/90} = 0.8\, I_{100}/T_{10/90}$ and between 30 and 90 % amplitude intercepts defined as $S_{30/90} = 0.6\, I_{100}/T_{30/90}$;

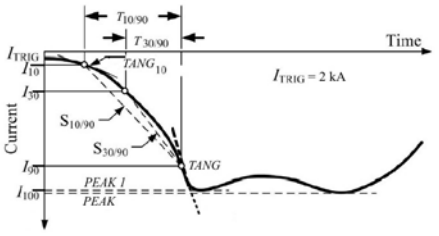

Fig. 3 – Current's waveform and definitions of front parameters for the first stroke in a negative downward flash, adapted from [15].

- two parameters for the rate of rising of current, *i.e.* the value at the beginning of the return stroke event, $TANG_{10}$, and the maximum rate of rising of the current on the front, *TANG*.

Especially for the first stroke, it was proved necessary to distinguish between the first peak of the current (I_{100} or *PEAK*1) and the second peak (*PEAK*) which can occur 5 – 10 μs later.

For the statistical analysis, a sample of 80 records of the first stroke waveform and a sample of 114 records of subsequent strokes waveforms have been set up, in time, by measurements performed on instrumented towers, [16].

d) Statistical distribution of waveform parameters. The parameters listed above form the components of a *p*-dimensional random vector $\mathbf{X} = (X_1, X_2, \ldots, X_p)^T \in \mathbf{R}^p$. The random vector distribution in the population under investigation may be characterized by its joint or multivariate probability density function (PDF) in (4):

$$F_{\boldsymbol{X}}(x) = F_{\boldsymbol{X}}(x_1,\ldots,x_p) = Prob(X_1 \le x_1,\ldots,X_p \le x_p) \tag{4}$$

A multivariate distribution is fully defined by the covariance matrix, a square matrix whose terms are the covariance between each pair of elements of a given random vector, and the matrix diagonal terms are variances, *i.e.*, the covariance of each element with itself.

Using the PDF in (4), marginal distributions of various types may be obtained by setting the arguments corresponding to unwanted variables equal to ∞. In this way, univariate distributions can be obtained for each component, (5), or bivariate distributions can be obtained for pairs of components, (6):

$$F_{X_i}(x_i) = F_{\boldsymbol{X}}(\infty,\ldots,\infty,x_i,\infty,\ldots x_p) = Prob(X_i \le x_i) \tag{5}$$

$$F_{(X_i,X_k)}(x_i,x_k) = F_{\boldsymbol{X}}(\infty,\ldots,\infty,x_i,\infty,\ldots\infty,x_k,\infty,\ldots x_p) = Prob(X_i \le x_i, X_k \le x_k) \tag{6}$$

As it results from the statistical analysis of the available waveforms sample, the marginal univariate distributions (5) of each of the random vector's components have lognormal PDFs whose parameters, *i.e.* location and shape parameters, can be found in [15, 17].

The present work is interested in the bivariate distribution (6) for two of the random vector's components, namely I_{100} and *TANG*. Both parameters have lognormal marginal univariate distributions with μ-location parameter

and σ-shape parameter given in Table 1. It is known that a lognormal random variable is a variable whose logarithm is normally distributed. The interdependence of I_{100} and *TANG* is described by the coefficient ρ of partial correlation. According to reference [15], for the first stroke, the partial correlation coefficient equals 0.430, while for the subsequent strokes the value equals 0.560.

Table 1

Estimated parameters for lognormal PDFs of I_{100} and *TANG*, [15]

			μ	σ_{ln}
First stroke	I_{100}	**[kA]**	ln(27.7)	0.4605
	TANG	**[kA/μs]**	ln(24.3)	0.5987
Subsequent strokes	I_{100}	**[kA]**	ln(11.8)	0.5365
	TANG	**[kA/μs]**	ln(39.9)	0.8520

μ-location parameter, σ_{ln}-shape parameter

The pair of primary random variables {*TANG*, I_{100}} with lognormal marginal PDFs will produce, by the transformations $x = \ln(TANG)$ and $y = \ln(I_{100})$, a pair of random variables {*x*, *y*}, with normal univariate marginal PDFs. Due to the existent correlation ($\rho \neq 0$), the random vector {*x*, *y*} has a bivariate normal joint PDF given by equation (7):

$$F_{(X,Y)}(x,y) = \frac{1}{2\pi\sigma_x\sigma_y\sqrt{1-\rho^2}}\exp\left[-\frac{Q(x,y)}{2\left(1-\rho^2\right)}\right]$$
$$Q(x,y) = \frac{(x-\mu_x)^2}{\sigma_x^2} - \frac{2\rho(x-\mu_x)(y-\mu_y)}{\sigma_x\sigma_y} + \frac{(y-\mu_y)^2}{\sigma_y^2}, \quad (7)$$

where μ_x, μ_y, σ_x, σ_y are the location and shape parameters for the marginal distributions of random variables *x* and *y* and ρ the correlation coefficient. The bivariate normal PDF can be visualized using the level surfaces or cross-sections of $F_{(X,Y)}(x, y)$; some of the significant cross-sections are plotted in Fig. 4. The cross-sections contours are closed curves whose positions and shapes are decided by the properties of the quadratic form *Q* (*x*, *y*) in equation (7).

The quadratic form *Q* (*x*, *y*) in equation (7) is an ellipse in its general form. To obtain the well-known parametric representation of the standard ellipse, two coordinates' transformations have been performed: (i) a translation of the origin to the center of dispersion of the bivariate distribution (μ_x, μ_y), (ii) a rotation with an angle α whose value may be computed using the general form's coefficients. It should be mentioned that the bivariate distribution function reported in Fig. 4 will prove to be an important tool to use in those lightning protection applications involving the joint effect of current crest value and current's derivative, such as prediction of the risk of failure for phase insulation under back-flashover conditions, assessment of surge performance of an earthing system or evaluation of induced voltages.

e) Lightning current waveform equation. In order to model the transients associated with a strike scenario, an analytical function is needed, capable of reproducing most of the lightning current's features. In the study undertaken, the equation proposed by Heidler in [19] has been used:

$$i(t) = \frac{I_0}{\eta}\frac{k^{10}}{1+k^{10}}exp\left(-\frac{t}{\tau_2}\right) \quad k = \frac{t}{\tau_1} \quad (8)$$

where I_0 is the current peak, η the correction factor of the current peak, τ_1 and τ_2 the time constants determining current rise- and current decay-time. The shape parameters η, τ_1 and τ_2 have been inferred given the time-to-peak (T_{CR}) and the time-to-half value (T_B) intended for the waveform. In the performed study, seven current's waveforms have been used, all with the same time-to-half value (20 μs) and different time-to-peak values (16-12-8-4-2-1-0.5 μs).

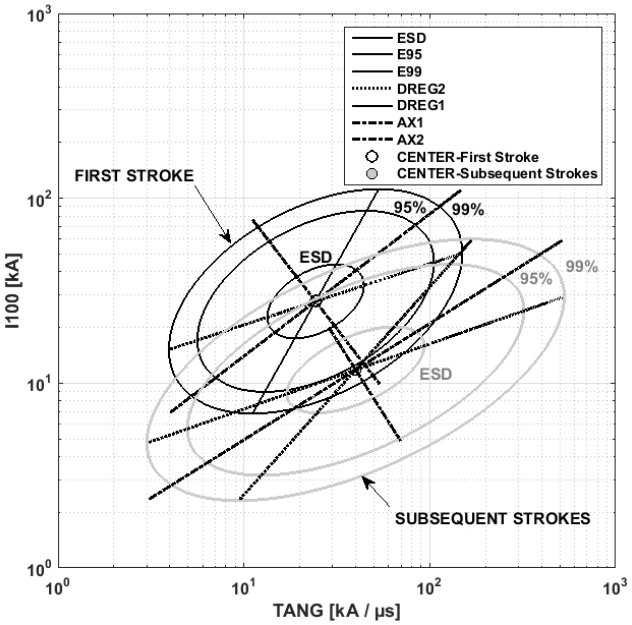

Fig. 4 – Visualization, using probability ellipses, of the bivariate normal distribution for the random vector {*x*, *y*} the equivalent of {ln (*TANG*), ln (I_{100})}. Both first and subsequent strokes are considered.

ESD – contour curve covering 39.5 % of all possible values of the underlying population, designated as population's concentration ellipse;
E95, E99 – contours curves containing 95 % and 99 % of all possible values of the underlying population, designed as confidence ellipses;
AX1, AX2 - major (AX1) and minor (AX2) principal dispersion axis of the standardized bivariate normal distribution;
DREG1, DREG2,- represent the locus for the means of conditional PDFs of *y* given *x* (DREG1) and *x* gave *y* (DREG2) respectively

5. CRITICAL CURRENTS CURVE

Early studies on flashover rate introduced the critical current concept in relation to the shielding failure event, being defined as the lowest crest value of the lightning current which produces a voltage at the phase-to-ground insulation terminals equal to the CFO, for a strike on the phase conductor at midspan. The critical current can be computed as

$$I_{critical} = 2\,\mathrm{CFO} / Z_{char}, \quad (8')$$

with Z_{char} – conductor surge impedance under corona discharge. As it can be noticed from (8'), any lightning current with the crest value higher than $I_{critical}$ will end in a flashover. Simulations of this scenario in ATP-EMTP have confirmed relation (8) as true. For OHL with rated voltages between 110 and 400 kV the magnitude of the critical current is in the range 3 to 8 kA.

In contrast to FO associated to shielding failure, in the case of a BFO, the voltage across line insulation has, in the first 1 to 6 μs, two wave contributors: the resistive voltage rise of the tower footing, and an "inductive" voltage added by the tower surge response. Therefore, in this case, both the crest value and the speed of rising of the current will determine the flashover condition. A condition that incorporates the influence of two independent continuous variables could be described by a plane curve which, in this particular case, should be delineated as *C* (*TANG*, I_{100},).

Each point of *C* represents the *minimal combination* of the crest and the maximum derivative values of the lightning current during a stroke event ended in a BFO. The curve divides the plane $\{TANG, I_{100}\}$ into two regions: the region below the curve in which the conditions for obtaining a BFO event are not met, the region above the curve in which the combination of $\{TANG, I_{100}\}$ values leads in each case to a BFO event. It should be noticed that such a curve exists for each of the possible strike scenarios.

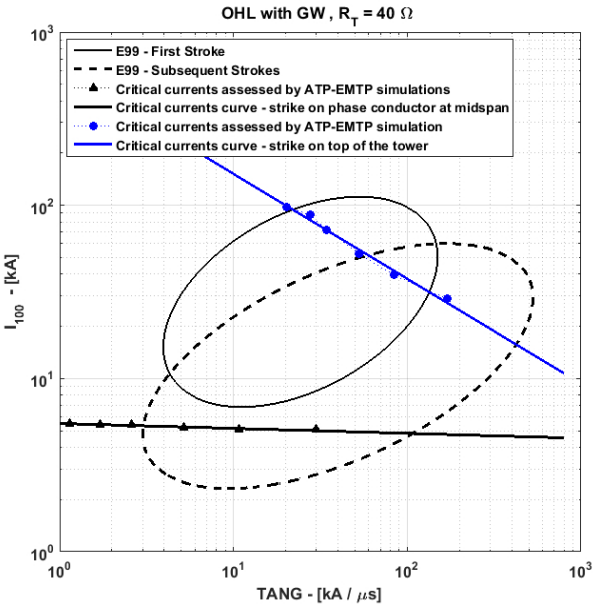

Fig. 5 – Critical current curves for two different strike scenarios:
- strike on the phase conductor at midspan followed by a FO
- strike on the top of the tower followed by a BFO

The visual illustration of the critical currents curve (CC-curve) concept can be followed in Fig. 5. The figure contains the E99 confidence ellipses which hold 99 % of the possible values of the pair of variables $\{TANG, I_{100}\}$ in the case of first and subsequent strokes respectively. The CC-curves for two different strike scenarios are superimposed over the ellipses mentioned above. The scenario chosen to explain the CC-curve concept was the lightning striking on the top of the tower. The corresponding CC-curve is, in log-log scale, a line with a negative slope, highlighting the fact that with the increase of the lightning current slope, represented here by the variable *TANG*, the peak value I_{100} necessary to ensure the conditions leading to a BFO decreases. In contrast with the scenario ended in a BFO, the second scenario considered, namely a shielding failure, generates a CC-curve in the shape of a practically horizontal line, pointing out the determining role of the crest value of the current in reaching the FO condition.

The CC-curves have been obtained using ATP-EMTP simulation of the relevant strike scenarios (see Fig. 1). The choice of the scenario decides the equivalent scheme of the simulated transient regime. For a given scenario, calculation of the transient regime initiated by the lightning strike has been performed using current's waveforms belonging to the family of waveforms described by equation (8). The current's waveforms used have been specified by two time-based parameters: the time-to-peak and the time-to-half value (see Section 4 point c).

Within the given scenario, the determination of the critical current corresponding to a given waveform consists in the repetition of the calculations, preserving the model and the waveform time parameters while changing the crest current's value at each use of ATP-EMTP. The query for a critical current starts at a lower crest value and continues increasing step by step until the first (and simplest) BFO occurs. The pairs formed by the critical current crest value (variable I_{100}) and the associated maximum value of the current's derivative (variable *TANG*) obtained following this procedure are represented in Fig. 5 as points marked with circles and triangles; they form the available data set based on which the CC-curve has been approximated.

The occurrence of a BFO has been decided by comparing the instantaneous values of the voltage across the insulator string with the U_d (T_d) characteristic (Section 3 point (b)). It has to be emphasized that the rise of the crest current's value above the assessed critical value activates more complex mechanisms of insulation flashover, affecting not only the insulator string(s) in the neighborhood of the point-of-strike but also in others remote areas, due to surge propagation and surge reflections at each tower.

In a first approach, the CC-curve was approximated by a regression line in the space of the transformed variables $\{\log(TANG), \log(I_{100})\}$ whose parameters, *a* and *b* respectively have been inferred from the discrete set of available data using the least squares technique:

$$\log(I_{100}) = a + b\ \log(TANG) + \varepsilon \tag{10}$$

where ε is a random variable N (ε; 0, 1).

6. INTRINSIC PROBABILITY OF DISRUPTIVE PHENOMENA

In the $\{TANG, I_{100}\}$ space, the confidence contours such as E99 in Fig. 5 cover, in the variables' space, the probable location of pairs of *TANG* and I_{100} variables observed during a first or subsequent stroke.

As already mentioned, the CC-curve separates the population $\{TANG, I_{100}\}$ into two regions:
- the region containing combinations $\{TANG, I_{100}\}$ which do not cause disruptive phenomena at the insulation terminals (region situated below the CC-curve),
- the region containing combinations $\{TANG, I_{100}\}$ which cause disruptive phenomena at the insulation terminals (region situated above the CC-curve).

Depending on the strike scenario, the disruptive phenomena produced when exceeding the CC-curve can be a direct (FO) or a back insulation flashover (BFO).

We define the *intrinsic probability of disruptive phenomena* as being that part of the confidence ellipse's area placed above the CC-curve associated with a given strike scenario. As it can be seen in Fig. 5, not only the first stroke current contributes to this probability; subsequent strokes can determine a disruptive phenomenon as well. The probabilities P_{PH}, P_T, P_{GW} introduced in Section 3 point (a) and Fig. 1 are assessed as intrinsic probabilities of exceeding the CC-curves generated by different strike scenarios. Following the analyzed strike scenario, the intrinsic probability of disruptive phenomena can be intrinsic BFO probability or intrinsic FO probability.

To evaluate the intrinsic BFO or FO probability we have applied to the quadratic form $Q(x, y)$ in equation (7) a sequence of affine transformations implying translation to the dispersion center, rotation and standardization, leading to a new bivariate distribution with the dispersion center (0, 0), standard deviations equal to 1 for both variables, and

correlation coefficient equal to 0. In practical terms, the confidence ellipses of the initially bivariate lognormal distribution (see Fig. 4) change into circles. The circle corresponding to an $E(P)$ confidence ellipse will have a radius C equal to the P-quantile of the chi-square distribution with 2 degrees of freedom (P – probability). For example if the confidence ellipse is traced for $P = 99.9$ % the radius of the corresponding circle is $C = \text{sqrt}(-2 \log(1 - P)) = 3.717$ p.u.

The critical currents curve undergoes the same sequence of transformations; the model (10) remains unchanged as the suite of applied transformations conserves the lines, but the parameters a and b will change incorporating the translation, rotation and standardization effects. For example, the final appearance, after transformations, of the confidence ellipses and the CC-curve for the top-of-tower strike scenario in Fig. 5 is the one illustrated in Fig. 6: the confidence ellipses for the first and subsequent strokes are both mapped on the same circle with the radius $C = 3.717$. Because the actual transformations undergone by the CC-curve differ, in numerical terms, from the first and subsequent strokes, the CC-curve becomes the line A1B1 when assessing the intrinsic probability of a BFO produced during a first stroke and A2B2 for subsequent strokes.

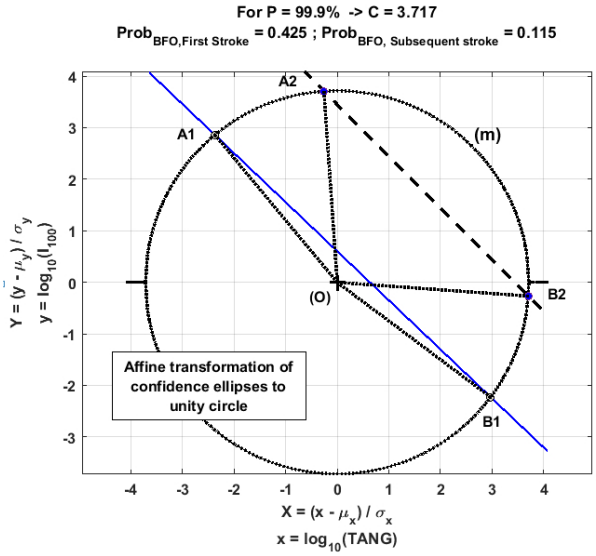

Fig. 6 Visualization of the intrinsic probability of disruptive phenomena generated by the top-of-tower scenario. Transformation of CC-curve generated by the top-of-tower strike scenario

The intrinsic BFO probability for first stroke events can be interpreted as the area bordered by the line segment A1B1 and the arc A1(m)B1, while the BFO probability for subsequent strokes events is the area bordered by the line segment A2B2 and the arc A2(m)B2. Values of these two intrinsic probabilities are given in Fig. 6. The calculation of these areas is elementary.

7. CASE STUDY

The line under analysis is a 220 kV rated voltage, single circuit line on supporting steel towers with a medium height of about 28 m and an Y top tower geometry, provided with 1x400/75 mm^2 Al-OL phase conductors. The phase-to-ground insulation consists of single suspension insulators strings with 16 glass insulators units.

The route of the line, depicted in Fig. 7 crosses a mountainous region reaching the altitude of 1500m. The lightning activity in the right-of-way of the line is assessed by the contour curves of the GDF which are also visible in Fig. 7. Annual average GDF values higher than 1.5 flashes /km^2/year have been observed in the area of the line's route on the southern side of the mountain. About 30 % of the line length is placed in a region where, during the winter, ice accretions on line's conductors, towers, and insulator strings occur frequently. The ice covering, combined with blizzard creates conditions for conductors galloping, with heavy consequences for the line's integrity. To reduce these risks, a part of the line is operated without grounding wires (total length of OHL section 18.6 km). The rest of the line is equipped with 2x70 mm^2 Ol-Zn grounding wires. Another particularity of the OHL under study is the high value of the soil resistivity (up to 1000 Ω·m for weathered rock) which makes the earthing resistances of the towers to have unusually high values.

The partial elimination of grounding wires, the high value of soil resistivity, and a relatively high lightning activity have led to an important number of line's outages. To improve this situation, several solutions have been considered:
(i) – restoring grounding wires in all spans regardless of the risk of having galloping conductor situations during the winter;
(ii) – decreasing the value of tower footing resistance by adding new electrodes to the existing ones;
(iii) – using line surge arresters (LSA).

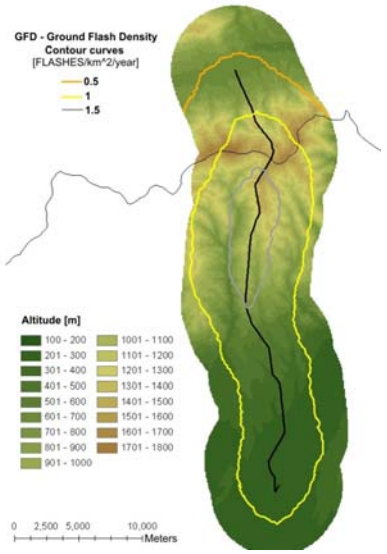

Fig. 7 Route of the studied OHL and contour curves of the observed average multiannual values for GFD, superimposed over the physical map of the region. Data have been provided by the Romanian Lightning Detection System

The method based on critical currents curves introduced above has been developed as a tool meant to establish an order of merit among the available solutions.

a) Modeling for lightning overvoltages calculations. Several guidelines of power components models recommended in lightning overvoltage simulations are available, starting with the ATP-EMTP theory book, [20]. The models developed over time, are well adapted to the peculiarities of this type of transient, namely the wide frequency range of the lightning current, inherited by the lightning overvoltages, which spans from 1 kHz to about 1 MHz. For this study, several transmission system schemes have been implemented in ATP-EMTP, one for each lightning strike scenario. As an example, the scheme used for the top-of-tower strike scenario is illustrated in Fig. 8. Each span of the line in the vicinity of the hit tower

was represented by a multiphase, untransposed, distributed frequency-dependent parameters line section (J. Marti model), three spans at each side of the point-of-strike. At each side of the above model, the line was adapted, to avoid reflections that could affect the overvoltages evolution in the neighborhood of the point-of-strike.

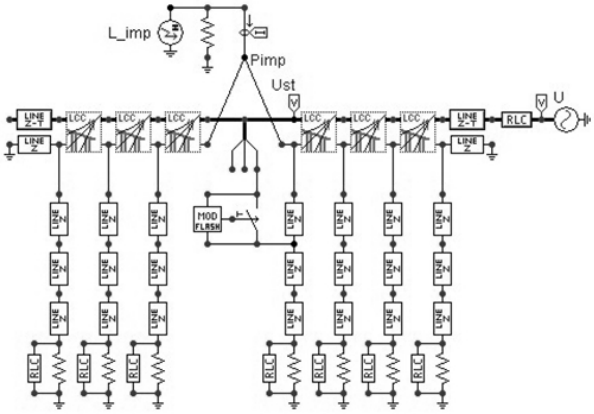

Fig. 8 Circuit scheme for lightning strike to tower top scenario simulation

For the towers' model, the single conductor line with constant distributed parameters has been adopted. It is the simplest model but sufficiently accurate for towers shorter than 30 m, [21]. The tower's footing resistance, (TFR), modelling is critical when studying the voltage conditions leading to BFO. In a first approximation, the tower footing resistance was represented by a RL series branch responsible for the transient behavior, in parallel with a second resistance equal to the earthing resistance of the grounding arrangement, computed for low frequency. Lightning is simulated by a current generator (L_imp in Fig. 8) which injects a current following the Heidler's law detailed in equation (8).

To close this presentation of the models adopted for the main components of the transmission system, it should be underlined that other, much complex models can be implemented, without changing the substance of the method based on critical currents' curve proposed in the present paper.

b) Simulations' results for different lightning strike scenarios. To obtain a detailed image of the OHL lightning performances, and to evaluate the effect of the different improvement measures available, 30 different scenarios have been implemented in ATP-EMTP. For this paper, only a part of these scenarios will be presented, a part that covers the analysis of the line section without grounding wires mentioned above. The final results of the analysis undertaken following the steps presented in the Sections 5 and 6 are summarized in Table 2, which contains, apart from the short description of the case and strike scenario, the CC-curve parameters *a* and *b* in equation (10), and the intrinsic probability of exceeding the CC-curve, *P*, which incorporates also the contribution of subsequent stokes.

To improve the lightning performance of this special line section, five solutions have been assessed as follows.

1) Adding GWs without other changes.

2) Adding GWs and supplementing the grounding electrodes at each tower to decrease the footage impedance towards 40 Ω.

3) Adding one-line surge arrester (LSA) on the central phase B at each tower of the line section without other changings.

4) Adding a LSA on each of the lateral phases A(C) at each tower of the line section without other changings.

5) Adding a LSA on each phase at each tower of the line section without other changings.

The investments required by the implementation increase from solution 1 to solution 5. In addition to the necessary investments, the adoption of solution 1 or 2 will implicitly lead to the increase of the risk of conductors galloping occurrences during the winter season.

Table 2

Critical currents curves and intrinsic probabilities of disruptive phenomena as a function of lightning strike scenarios taken into account in each of the protection solutions (cases) under study.

Case	Strike scenario	*a*	*b*	*P*
OHL without GW TFR = 80 Ω	phase B (or A or C) at midspan	0.688	-0.012	0.999
	top of tower	1.439	-0.324	0.798
OHL with GW TFR = 80 Ω	phase B (or A or C) midspan–shielding failure	0.744	≅ 0	0.969 (*)
	top of the tower	2.056	-0.292	0.356
	GW at midspan	3.548	-1.246	0.356
OHL with GW TFR = 40 Ω	phase B (or A or C) midspan -shielding failure	0.740	≅ 0	0.969 (*)
	top of the tower	2.646	-0.511	0.212
	GW midspan	5.183	-2.041	0.263
OHL without GW TFR = 80 Ω 1 x LSA on central phase (S)	phase B midspan	3.835	-1.424	0.354
	phase A (C) midspan	0.692	-0.002	0.999
	top of the tower	1.616	-0.193	0.571
OHL without GW TFR = 80 Ω 2 x LSA on phases R and T	phase B at midspan	0.737	-0.029	0.969
	phase A (C) midspan	2.275	-0.448	0.368
	top of the tower	1.969	-0.158	0.267
OHL without GW TFR = 80 Ω 3 x LSA on each phase at each tower	-	-	-	0.000
	-	-	-	0.000
	-	-	-	0.000

(*) – For the shielding failure scenario only the contribution of first strokes has been considered when computing the intrinsic probability *P*.
TFR-tower foot resistance, GW – ground wire, LSA – line surge arrester

c) Total flashover rate calculation. Each of the lightning strikes collected by the line, N_S, will lead to a disruptive event (FO or BFO) following the models which make the subject of diagrams in Fig. 1. The relationship between the total flashover rate N_D in flashovers/100 km/year and N_S can be estimated as follows:

- for the OHL without GW

$$N_D = N_S \left\{ p \cdot P_T + (1-p) \cdot \left(q \cdot P_B + (1-q) \cdot P_{A(C)} \right) \right\} \quad (11)$$

- for the OHL with GW

$$N_D = N_S \left\{ P_{SF} \cdot P_{PH} + (1-P_{SF}) \cdot \left(p \cdot P_T + (1-p) \cdot P_{GW} \right) \right\} \quad (12)$$

The quantities in equations (11) and (12) have been explained in Section 3 point (a) and Fig. 1a and b. They form two groups: (*i*) probabilities that depend mostly on the OHL geometry (*p*, *q* and P_{SF}), and (*ii*) intrinsic probabilities of disruptive phenomena introduced in section 6 (P_{PH}, P_B, $P_{A(C)}$, P_T, P_{GW}). As already discussed, for each protection solution considered (case), the intrinsic probabilities depend on the strike scenario; their values are given in Table 2 in relation with the associated CC-curves and regrouped in Table 3 according to the scenarios analyzed.

In the equations that evaluate the total flashover rate, the least reliable terms are in fact the probabilities *p* and *q* in the model of OHL without GW and respectively *p* and P_{SF} in the model for OHL with GW. To obtain more realistic values for these quantities, use of electrogeometric models

is highly recommended.

Table 3
Intrinsic probabilities for protection solutions (cases) under study regrouped according to the strike scenarios considered

Case \ Strike scenario	P_B	$P_{A(C)}$	P_T	P_{GW}
OHL without GW, TFR = 80 Ω	0.999	0.999	0.798	-
OHL with GW, TFR = 80 Ω	0.969	0.969	0.356	0.356
OHL with GW, TFR = 40 Ω	0.969	0.969	0.212	0.263
OHL without GW, TFR = 80 Ω 1 x LSA on central phase B	0.354	0.999	0.571	-
OHL without GW, TFR = 80 Ω 2 x LSA on lateral phases A(C)	0.969	0.368	0.267	-
OHL without GW, TFR = 80 Ω 3 x LSA on each phase	0	0	0	-

Because we are more interested in establishing an order of merit among the different protection solutions, in a first approach, the following values have been assigned to p, q and P_{SF}: $p = 0.3$, $q = 0.4$, $P_{SF} = 0$ (the OHL has two GWs placed so that the exposure arc of the lateral phases is equal to zero). It should be noticed that all three probabilities quoted above are involved in the number of strikes collected by the OHL's components and not in the completion of an event in FO or BFO. Table 4 includes values for N_D assessed with equations (11) and (12). The flashes collection rate, N_S, has been evaluated for a GFD equal to 1.5 flashes/km^2/year and equals 30.5 flashes/100km/year. Table 4 includes also the number of disruptive events (FO and BFO) to be expected for the special OHL's section under study which is 18.6 km in length, N_D*.

Table 4
Flashover rate for 100 km (ND) and for the special section

Cases	N_D [100 km/year]	N_D^* [18.6 km/year]
(0) OHL without GW, TFR = 80 Ω (REFERENCE)	28.6	5.3
(1) OHL with GW, TFR = 80 Ω	10.8	2.0
(2) OHL with GW, TFR = 40 Ω	7.5	1.4
(3) OHL without GW, TFR = 80 Ω 1 x LSA on central phase B	21.0	3.9
(4) OHL without GW, TFR = 80 Ω 2 x LSA on lateral phases A(C)	31.0	5.8
(5) OHL without GW, TFR = 80 Ω 3 x LSA on each phase	0	0

As (0) case is the reference one, the solutions considered to improve the lightning performance of the special OHL section have the following order of merit (5)-(2)-(1)-(3)-(4).

8. **CONCLUSIONS**

The paper introduces, in Section 5, and makes use of the concept of *critical currents' curve* by means of which it can be expressed the joint influence of two parameters of the lightning current, namely the crest value (I_{100}) and the rate of rising (*TANG*), on the voltage values at the insulation terminals. The critical currents' curve associated with a given strike scenario can be established by simulations in ATP-EMTP or other dedicated software. The position of the critical currents' curve in relation to the confidence ellipses of the bivariate *TANG*-I_{100} distribution, highlights the area containing those pairs of current's crest and rate of rising values able to produce a disruptive phenomenon (FO or BFO) to the insulation terminals. For a specified OHL structure, each strike scenario has its own critical currents' curve.

The second concept introduced is that of the *intrinsic probability of disruptive phenomena* (BFO or FO), defined in Section 6, by which the capability of a given strike scenario to produce a disruptive phenomenon at the insulation terminals is assessed.

For a given OHL situation (case), the intrinsic probabilities of disruptive phenomena related to every possible strike scenario have been combined using equations (11) and (12) to obtain the total flashover rate N_D. The quoted equations contain weighting factors that take into account the influence of the OHL geometry on the distribution of lightning strikes among the line's components.

The case study carried out, highlights the sensitivity of the proposed method, and therefore its ability to produce a clear order of merit among the available lightning protection solutions. It should be noted that the proposed method can handle also lightning protection solutions of OHL based on line surge arresters.

Received on November 7, 2020

REFERENCES

1. E. R. Whitehead, *Protection of transmission lines*, chapter 22 in *Lightning*, R. H. Golde, Academic Press, 1977.
2. J. G. Anderson, *Transmission Line Reference Book - 345 kV and Above*, Second Edition, 1982, Chapter 12, Electric Power Research Institute, Palo Alto, California.
3. A. J. Eriksson, *The Incidence of Lightning Strikes to Transmission Lines*, IEEE Trans. on Power Delivery, **PWRD-2**, *3*, pp. 859-870, July 1987.
4. * IEEE WG on Estimating Lightning Performance of Transmission Lines; *A Simplified Method for Estimating Lightning Performance of Transmission Line*, IEEE Trans., **PAS-104**, *4*, pp. 919-932, April 1985.
5. * IEEE WG Report, *Estimating the Lightning Performance of Transmission Lines II - Updates to Analytical Models*, IEEE Trans. on Power Delivery, **PWRD-8**,.*3*, pp.1254-1267, July 1993.
6. * IEEE Std. 1243-1997, *IEEE Design Guide for Improving the Lightning Performance of Transmission Lines*.
7. * CIGRÉ WG 33-01, *Guide to Procedures for Estimating the Lightning Performance of Transmission Lines*, CIGRÉ Technical Brochure, Nr. 63, October 1991.
8. D. Loudon and others, *A compact 420 kV line utilizing line surge arresters for areas with low isokeraunic levels*. CIGRE Session Paris, paper 22/33/36-08, 1998.
9. M. Mobedjina, L. Stenström, *Improved transmission line performance using polymer – housed surge arresters*. CEPSI seminar, Manila, Philippines, October 2000.
10. * *Use of surge arresters for lightning protection of transmission lines*, CIGRE WG C4.301, Technical brochure, 2010.
11. R. B. Anderson et al, *Lightning and thunderstorm parameters*, Lightning and Power Systems, London, IEE Conf. Publ. no. 236
12. A. J. Eriksson, *The incidence of lightning strikes to power lines,* IEEE Trans on Power Delivery, **2**, *3*, July 1987, pp. 859-870.
13. V. A. Rakov, M. A. Uman, *Lightning. Physics and Effects*, Cambridge University Press, 2003.
14. * *Parameters of lightning strokes: A review*, IEEE Trans. on Power Delivery, **20**, *1*, pp. 346-358, January 2005.
15. R. B. Anderson, A. J. Eriksson, *Lightning parameters for engineering application,* Electra, **69**, March 1980, pp. 65-103.
16. K. Berger, *Wissenschaftlicher Bericht über die Blitzforschung auf dem San Salvatore in den Jahren1963...1971*, (8702 Zollikon).
17. * CIGRE WG 33-01, *Guide to procedures for estimating the lightning performance of transmission lines*, 1991.
18. * IEEE Standard 1243-1997, *IEEE Guide for Improving the Lightning Performance of Transmission Lines.*
19. F. Heidler, J. M. Cveticic, B. V. Stanic, *Calculation of Lightning Current Parameters,* IEEE Transactions on Power Delivery, **14,** *2*, April 1999.
20. Eiichi Haginomori, Tadashi Koshiduka, Junichi Arai Hisatochi Ikeda, *Power System Transient Analysis: Theory and Practice using Simulation Programs (ATP-EMTP)*, John Wiley & Sons, Inc., New York – London – Sydney, 2016.
21. A. R. Hileman, *Insulation Coordination for Power Systems*. New York: Marcel Dekker, 1999.